Global Sensitivity Analysis of Distance Protection Performance for Submarine Transmission Systems

Mirko Ginocchi[1], Thanakorn Penthong[1], Muhammad Zeeshan Khattak[1], Alexander Och[2], Ferdinanda Ponci[1], and Antonello Monti[1,3]

[1] *Institute for Automation of Complex Power Systems, RWTH Aachen University, 52064 Aachen (DE)*

[2] *Institute of High Voltage Equipment and Grids, Digitalization and Energy Economics, RWTH Aachen University, 52068 Aachen (DE)*

[3] *Fraunhofer FIT, Center for Digital Energy, 52068 Aachen (DE)*
**Corresponding Author Email: mirko.ginocchi@eonerc.rwth-aachen.de*

Abstract

The distance protection performance depends on the accurate definition of the relay settings. These are computed from the line impedance, which needs, for its calculation, various parameters (such as geometry and cross-section of the cable, soil properties); their uncertainty might jeopardize the performance of the fault location algorithm. Via global sensitivity analysis, this paper investigates which are the main drivers of the distance protection performance in a submarine transmission system. The results underscore the need to better characterize the earth resistivity (via direct or indirect measurement), and the risk of the common practice to adopt "default" values for it. Also, the cable model of the EMT software tools used to compute the line impedance can be, already per se, an error source for distance protection algorithms.

1 Introduction

Investments in technical infrastructures to connect international electric grids and the boost to the sustainable adoption of renewable energy generated by offshore wind parks has been leading to massive investment in HVDC submarine transmission lines [1]. However, the cost effectiveness of DC technology over AC is less noticeable for long distances, and existing HVAC submarine lines are still widely adopted for short-range connection (e.g., up to 150 km) [2]. Submarine cables are laid on the seabed and connected to the transmission system on the mainland via underground cables at both ends. Notwithstanding mechanical precautions against damage and reinforced cable armoring, they can experience internal breakdown due to human activities and natural factors [3]. This can ultimately lead to expensive and widespread power outages [4].

For HVAC submarine cables, which are the focus of this paper, transmission system operators (TSOs) often use the distance protection as the main protection function, due to its simplicity, selectivity, and dependability. When other solutions are chosen (e.g., line differential protection), distance protection still represents the back-up function that acts as soon as failure in the communication happens. The distance protection function is implemented in impedance-based fault location (IFL) algorithms, which estimate the distance to the fault on the transmission line as follows: when a fault occurs at m kilometers away from the near-end substation, an intelligent electronic device (IED), such as a digital relay, captures the voltage and current waveforms, and measures the apparent impedance Z_{app} between the IED and the fault location. The Z_{app} is compared to the reference line impedance Z_L; if $Z_{app} < Z_L$, the IED triggers a signal to the appropriate circuit breaker to isolate the faulted line section, and the absolute distance to the fault ($\widehat{m}$) is measured. Especially for submarine cables, crucial is estimating the location of the fault in an accurate way (i.e., with a small error $\widehat{m} - m$), since the time to find and repair the fault becomes particularly critical [4].

Various IFL algorithms have been proposed in the literature [5]. Regardless of their working principles and applicability boundaries, they all have in common that their proper operation and accuracy depend, among the others, on the correct calculation of the reference values of the sequence components of Z_L, in terms of zero-sequence Z_{0L} and positive-sequence Z_{1L}. In fact, Z_{0L} and Z_{1L} are adopted for both setting up the IED's protection zones and computing the zero-sequence compensation factor (k_0) to estimate Z_{app} in the case of line-to-ground faults [6]. Remarkably, Z_{0L} and Z_{1L} are usually not the outcome of some measurement process, but rather of a calculation [7]. To this scope, electromagnetic transient (EMT) software tools are routinely employed [7, 8], which have dedicated cable models to ultimately compute the reference Z_{0L} and Z_{1L}, and hence the IED settings. To yield Z_{0L} and Z_{1L}, various parameters have to be specified, such as the geometrical configuration of the line (e.g., x-y coordinates of each conductor, burial depth of the cable system), the cable cross-section (e.g., inner and outer radii of each conductor), and properties of the surrounding medium (e.g., the earth resistivity (ρ)) [8, 9]. Nominal values are used for these parameters; yet, they are inevitably affected by uncertainties, due to e.g., the tolerance of the geometrical data provided by the cable manufacturers, or the inaccurate knowledge of ρ, for which the common practice is to adopt the "default" value of 100 Ωm for the whole transmission line [5, 7]. Owing to these uncertainties, the fault location measured by the IED might differ from the true one; such degradation of the IFL algorithm accuracy

ultimately undermines the timely and targeted intervention of the repair vessels and the quick restoration of the power supply after de-energization of the system [4].

To characterize how, and to what extent, various uncertainty sources affect the IED performance, Sensitivity Analysis (SA) is a key tool [10]. Few works exist that employ SA in the transmission system protection, such as [5], [11], and [12]. Ref. [5] investigates the effect of different sources of error (e.g., load current, fault resistance, ρ, etc.) in one- and two-ended IFL algorithms, yet with no specific focus on submarine transmission lines. Ref. [11] studies the impact of k_0 on the IED accuracy for single-line-to-ground (SLG) faults; yet, no systematic analysis of which factors primarily influence k_0 (and hence the relay accuracy) is done. Ref. [12] assesses the sensitivity of travelling-wave differential protection for HVDC transmission lines to the error in cable model parameters, though disregarding the fault location accuracy. From the methodological viewpoint, [5], [11], and [12] conduct one-at-a-time SA [10], which assesses the effect of each uncertainty source, individually, on specific performance metrics around a nominal condition. Owing to its restricting assumptions, one-at-a-time SA neither provides a complete picture of the distance protection sensitivity, nor reliably ranks the uncertain parameters in terms of relative importance; this hinders the effective identification of which uncertain parameters mostly impact the fault location algorithm accuracy and, hence, would be worth better characterization. Besides, when multiple uncertainty sources are simultaneously considered as in [13], only the effect of fault-related characteristics (e.g., location, resistance, inception angle, and type of the fault) is investigated on the distance protection performance, while assuming "perfect" knowledge of the line parameters.

The inaccurate computation of the line impedances, especially Z_0, has been already identified as the main bottleneck jeopardizing the performance of IFL algorithms [14]. Yet, this paper goes one step further by investigating which are the main factors driving the accuracy of the line impedance, and, hence, of the relay settings. Focus is put on the adopted cable model, the cable cross-section, the cable geometrical configuration, and the soil properties, to provide TSOs with recommendations for corrective actions and research directions. To this scope, variance-based SA (VBSA) is adopted [10], which is a global SA (GSA) technique that overcomes the limitations of one-at-a-time SA and allows to trustworthily capture the sensitivity behavior of the performance of the IFL algorithm.

The novel contributions of this paper are: (1) the SA of the IFL algorithm performance to the uncertainty of various parameters—related to the cable model, cable geometrical configuration, cable cross-section and ρ—via VBSA, when distance protection IEDs are used in a submarine transmission system; (2) the demonstration that the cable model of EMT software tools used to compute the line impedance might, already on its own, represent a source of error affecting the performance of IFL algorithms; (3) the development of a test set-up which consists of an hardware-in-the-loop (HIL) connection of a real-time simulator, an amplifier and an IED, interfaced with script-based routines to implement the Monte Carlo Simulation (MCS) and the VBSA of the IFL algorithm. Although the focus is specifically on distance protection for submarine cables, this paper ultimately provides TSOs with replicable guidelines to conduct thorough SA studies to test the performance of alternative protection functions (e.g., line differential) or consider various uncertainty sources of interest (e.g., generator in-feed effect, transmission line configuration, communication-related parameters).

2 Background on distance protection

In this section, the essential principles of the distance protection are provided; more details can be found e.g., in [6].

The distance protection function is primarily used to detect abnormal situations in the transmission system, and isolate faulty sections from it to prevent equipment damage. Its operation is based on the apparent impedance Z_{app} of the line, measured at the IED location, which is compared with the reference impedance Z_L. In the case of the most frequent type of faults, i.e., SLG faults, Z_{app} is computed as

$$Z_{app} = \frac{V_\phi}{I_\phi + k_0 I_\phi}, \tag{1}$$

where V_ϕ and I_ϕ are the measured voltage and current of the faulted phase ϕ (i.e., A, B, or C), and

$$k_0 = \frac{Z_{0L} - Z_{1L}}{3Z_{1L}} \tag{2}$$

The fault location $\widehat{m}$ recorded by the IED is computed as

$$\widehat{m} = \frac{|Z_{app}|}{|Z_{1L}|}, \tag{3}$$

where $|\cdot|$ is the complex magnitude operator.

3 Background on VBSA

In this section, the main mathematical details of the VBSA are provided; more details can be found e.g., in [10].

In generic terms, the IFL algorithm performance can be modeled as $y = \mathbf{f}(\mathbf{u})$, where: y is the output/metric of interest (scalar for convenience) that describes the distance protection performance; $\mathbf{u}$ is the vector of the d parameters $\{u_i\}_{i\in\{1,\dots,d\}}$ used to compute Z_{0L} and Z_{1L} needed for the IED settings. The components of $\mathbf{u}$ are uncertain and assumed to be independent random variables, each with a specific Probability Density Function (PDF). In this work, VBSA is adopted to apportion the uncertainty of the metric y to the d uncertain parameters, so to identify those having the highest impact on the IFL algorithm performance. In theoretical terms, VBSA decomposes the variance $Var(y)$ as

$$1 = \sum_i S_i + \sum_i \sum_{i<j} S_{ij} + \dots + S_{1\dots d} \tag{4}$$

where:

$$S_i = \frac{Var_{u_i}(\mathbb{E}_{\mathbf{u}_{\sim i}}[y|u_i])}{Var(y)}, \tag{5}$$

$$S_{ij} = \frac{Var_{u_i,u_j}(\mathbb{E}_{\mathbf{u}_{\sim ij}}[y|u_i,u_j])}{Var(y)} - S_i - S_j, \tag{6}$$

and so on for higher order terms [10]. $\mathbb{E}$ is the expected value, the subscripts of $\mathbb{E}$ and Var define the inputs over which the operators are taken, and $\mathbf{u}_{\sim i}$ and $\mathbf{u}_{\sim ij}$ indicate the removal of the input u_i and the inputs pair $\{u_i, u_j\}$ from $\mathbf{u}$, respectively.

The term S_i ($i \in \{1, ..., d\}$) is the first order Sobol' Sensitivity Index (SI), which quantifies the individual effect of each input u_i on $Var(y)$; the term S_{ij} ($i \in \{1, ..., d\}, j \in \{1, ..., d\} \setminus i$) is the second order Sobol' SI, which quantifies the interactive effect of u_i and u_j on $Var(y)$; and so on, up to the d-th order Sobol' index $S_{1...d}$. Also, the total effect SI T_i of u_i is:

$$T_i = S_i + \sum_{j=1, j\neq i}^{d} S_{ij} + ... + S_{1...d} = \frac{\mathbb{E}_{\mathbf{u}_{\sim i}}(Var_{u_i}(y|\mathbf{u}_{\sim i}))}{Var(y)}, \quad (7)$$

which quantifies the amount of $Var(y)$ due to all the contributions of u_i, including its interactive effects with other inputs of $\mathbf{u}_{\sim i}$; e.g., if $d = 3$, $T_2 = S_2 + S_{12} + S_{23} + S_{123}$. The Sobol' SIs of any order, e.g., S_i, S_{ij}, and the total effect SIs T_i are referred to as variance-based SIs.

The application of VBSA to study the IFL algorithm performance consists of the following steps: (a) identify the output/metric of interest y as well as the d uncertain inputs subject of the VBSA; (b) define the PDFs of the inputs to describe their uncertainty/variability; (c) for all the inputs, sample N values within their PDFs to build the input matrix $\mathbf{U}$ of size $[N, d]$; (d) perform a MCS of the IFL algorithm with the N input values' combinations of $\mathbf{U}$; (e) with the input matrix $\mathbf{U}$ and the N output values of y, estimate the variance-based SIs to assess the sensitivity of the IFL algorithm performance to the d uncertain parameters.

4 Test set-up

Fig. 1 depicts the HVAC power system under study, which consists of two land 115 kV single-core cable sections [15] (referred to as UG_1 and UG_2) and a 115 kV multi-core submarine cable connected in between [16]. The transmission line, whose total combined length is 54 km, connects the mainland (substation A) with an island (substation B). The IED where the IFL algorithm is implemented is at the near-end substation.

The developed test set-up is represented in Fig. 2, and it consists of two parts. On the right side (cyan box), the real-time simulator, the amplifier, and the IED under test are connected in HIL. On the left side (yellow box), script-based routines are interfaced with the HIL platform to perform various tasks, such as the MCS and the VBSA of the IFL algorithm, as well as the computation of the sequence impedances with the two approaches of Section 6. In both of these modelling approaches, the Z_{0L} and Z_{1L} values, once computed, are then fed to the real-time simulator to simulate the fault condition. Although specifically developed for the scope of this work, the overall test set-up can be straightforwardly replicated to conduct SA studies for other protection functions and/or accounting for different parameters of interest.

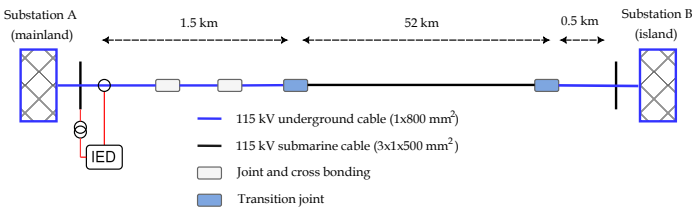

Figure 1: Single line diagram of the power system under study.

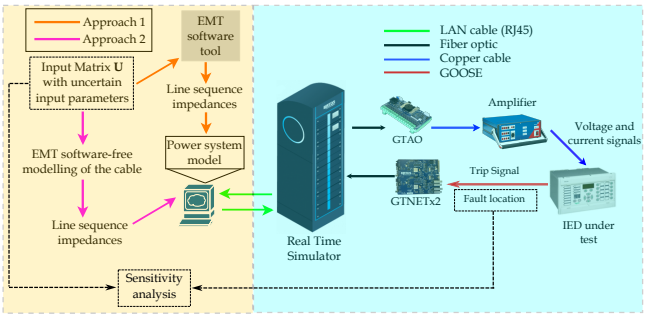

Figure 2: Test set-up developed for this work.

5 VBSA instantiation

The VBSA steps of Section 3 are instantiated as follows.

(a) The error $\epsilon = \widehat{m} - m$ is the metric for the IFL algorithm performance: the higher ϵ (in absolute value), the worse the performance. The parameters subject of the SA are listed in Table 1. They consist of geometrical data (e.g., coordinates of the land cables), cable cross-section (e.g., conductor radius, thickness of screen layers), ρ of the soil types which the cable sections are buried in (for UG_1 and UG_2 sections) or laid on (for the submarine section), and the location of the fault.

(b) The nominal values and the uncertainty of the parameters are derived by resorting to various sources, such as literature works addressing the same topic [12, 17] and cable manufacturers' data sheets [15, 16].

(c) The quasi-random Sobol' sampling strategy is adopted to generate $N = 2048$ combinations of $\mathbf{u}$.

(d) The N-size MCS of the IFL algorithm is performed by running the test set-up of Fig. 2 at all the rows of the input matrix $\mathbf{U}$ to record how the distance protection performance (in terms of ϵ) is affected by the uncertainty in $\mathbf{u}$. One MCS run is performed as follows: at each n^{th} test ($n = 1, 2, ..., N$), an SLG fault is applied in the power system at a random location m_n with the n^{th} combination of parameters $\mathbf{u}$; the fault location $\widehat{m}_n$ recorded by the IED is sent via GOOSE to the real-time simulator; the error ϵ between $\widehat{m}_n$ and m_n is computed.

(e) By using the input matrix $\mathbf{U}$ and the N values of fault location errors ϵ obtained from (d), the variance-based SIs are computed based on [18].

6 Cable specifications and models

In this section, the cable specifications are reported and the adopted cable modelling approaches are described.

The two land cables (UG_1 and UG_2 in Fig.1) are single-core cables laid in a flat formation with cross-section of 800 mm^2, whereas the submarine cable is a multi-core cable with cross-section of 500 mm^2. Fig. 3 depicts the cross-sections of both land and submarine cables; both cable types are characterized by various screen layers, such as conductor and insulator screen and semiconducting layer.

Previous works [2,8] have underscored that the cable models of the adopted EMT software tools might have shortcomings in characterizing some features of the real cable structure. Hence, this work considers two different cable modelling approaches to compute Z_{0L} and Z_{1L}. This is done to evaluate if the cable model used to compute Z_{0L} and Z_{1L} might be, already on its own, an uncertainty source potentially impacting the IED settings' accuracy and, hence, the IFL algorithm performance, irrespective of "external" uncertainties. In the modelling approach 1 (orange arrow in Fig. 2), the cable model of an EMT software is used to derive Z_{0L} and Z_{1L} for every n^{th} combination of the parameters. In particular, DigSILENT PowerFactory is used, in this work, as representative of EMT software tools. Even if the real cable configuration provided by the manufacturers involves many insulator and semiconducting screens (cf. Fig. 3), the PowerFactory cable model neglects some of them, assuming them to have no impact on Z_{0L} and Z_{1L}. In the modelling approach 2 (magenta arrow in Fig. 2), the Z_{0L} and Z_{1L} values are instead "EMT software-free": they are not computed using the EMT software cable model, but, instead, by reconstructing the cable model starting from the real cable characteristics. As the cable self impedance is inversely proportional to the geometric mean radius (GMR), modelling the cable with all the screen layers makes the GMR increase. This ultimately causes the self impedance to have a smaller value than that computed via the PowerFactory cable model. The impact of both cable modelling approaches on the IFL algorithm performance is assessed in Section 7.1.

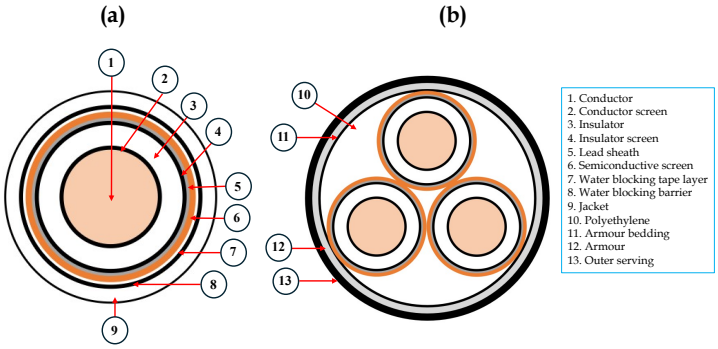

Figure 3: Cross-sections of (a) land and (b) submarine cables.

7 Test results

This section reports the test results of various analyses. Section 7.1 discusses the impact of the two cable modelling approaches on the IFL algorithm performance. Section 7.2 presents the SA of the IFL algorithm when the EMT software-free cable modelling approach is adopted.

7.1 Distance protection performance based on the cable model

To evaluate the IFL algorithm performance with the two above-mentioned cable modelling approaches, the MCS of the IFL algorithm is run by simulating an SLG fault at the fixed location of 30 km away from the near-end substation (i.e., in the submarine section). In both approaches, the parameters used to compute the sequence impedances are affected by the same uncertainty as described by the PDFs of Table 1.

The results of the IFL algorithm performance, in terms of fault location error, are shown in Fig. 4, when the sequence impedances are computed with and without the EMT software cable model (orange and magenta histograms, respectively). In the first case, the fault location error has a variability of around 2.5 km, with values of ϵ in the range $[1.5, -0.5]$ having almost equal probability. In the second case, the variability of the fault location error is way smaller, and the central tendency value of ϵ is localized around -0.6 km. Such result clearly points out that, if the cable model available in EMT software tools is not compatible with the real cable configuration (cf. Fig. 3), the EMT software cable model used to compute Z_{0L} and Z_{1L} might, already on its own, undermine the IFL algorithm accuracy. If the dependency from EMT software tools is dropped, "externally" computing the line impedances with a cable model that fully reflects the real cable configuration can help define more precise IED settings. Besides, from the histograms of Z_{0L} and Z_{1L} in both approaches (not shown here for brevity), it turns out that, as expected, the accuracy of Z_{0L} is smaller than Z_{1L}, signalizing that the main source of error in the IFL algorithm is due to the inaccurate estimation of Z_{0L} used to compute k_0.

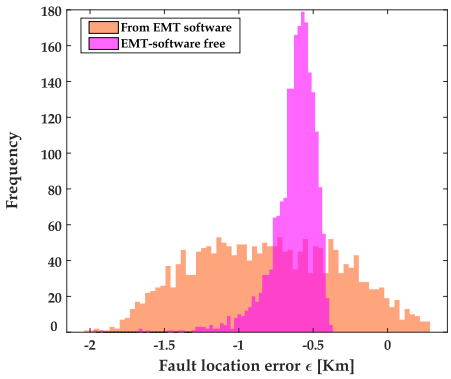

Figure 4: Performance of the IFL algorithm with the cable modelling approach 1 (orange) and 2 (magenta).

7.2 SA of distance protection performance

As seen in Section 7.1, the EMT software-free modelling of the cable characteristics (approach 2) allows the IFL algorithm to have better performance than the cable model of the EMT software (approach 1). Thus, in this section, the SA of the distance protection performance to the parameters of Table 1 is run exclusively for approach 2.

In reality, the distance protection performance depends also on the fault location (see e.g., [13]). Thus, beside the uncertainty in the cable geometry, in the cable cross-section and in ρ, the SA performed next includes the randomness of the fault location itself. Hence, at each MCS run, an SLG fault is simulated at a random location m sampled within the uniform PDF, whose lower and upper bounds correspond to the location of the near- and far-end substations, respectively (cf. last row of Table 1).

Table 2 reports the SA results considering all the 35 parameters, in terms of variance-based SIs and their confidence intervals. The IFL algorithm performance (cf. magenta his-

Table 1: Parameters subject to the SA.

	Name	Description	Units	Nominal value	Range	% Variation	Reference
Land cable (UG_1–UG_2)	u_1, u_{23}	Radius of the conductor	mm	17	[16.15, 17.85]	± 5%	[12, 15]
	u_2, u_{24}	Thickness of the conductor screen layer	mm	1.5	[1.425, 1.575]	± 5%	[12, 15]
	u_3, u_{25}	Thickness of the cross-linked polyethylene insulator	mm	16	[15.2, 16.8]	± 5%	[12, 15]
	u_4, u_{26}	Thickness of the semiconducting screen	mm	1.5	[1.425, 1.575]	± 5%	[12, 15]
	u_5, u_{27}	Thickness of the lead sheath	mm	3.5	[3.325, 3.675]	± 5%	[12, 15]
	u_6, u_{28}	Earth resistivity (dry inland soil)	Ωm	–	[20, 1000]	–	[17]
	u_7, u_{29}	x_1 coordinate of the cable	m	-0.5	[-0.475,-0.525]	± 5%	[12, 15]
	u_8, u_{30}	x_2 coordinate of the cable	m	0	[-0.05, 0.05]	± 5%	[12, 15]
	u_9, u_{31}	x_3 coordinate of the cable	m	0.5	[0.475, 0.525]	± 5%	[12, 15]
	u_{10}, u_{32}	y_1 coordinate of the cable	m	0.75	[0.5, 1]	± 5%	[12, 15]
	u_{11}, u_{33}	y_2 coordinate of the cable	m	0.75	[0.5, 1]	± 5%	[12, 15]
	u_{12}, u_{34}	y_3 coordinate of the cable	m	0.75	[0.5, 1]	± 5%	[12, 15]
Submarine cable	u_{13}	Radius of the conductor	mm	13.25	[12.59, 13.91]	± 5%	[12, 16]
	u_{14}	Thickness of the conductor screen layer	mm	2	[1.9, 2.1]	± 5%	[12, 16]
	u_{15}	Thickness of the XLPE insulator	mm	15	[14.25, 15.75]	± 5%	[12, 16]
	u_{16}	Thickness of the semiconducting screen	mm	1.5	[1.425, 1.575]	± 5%	[12, 16]
	u_{17}	Thickness of the lead sheath	mm	2.1	[1.995, 2.205]	± 5%	[12, 16]
	u_{18}	Thickness of the semiconducting polyethylene screen	mm	2	[1.9, 2.1]	± 5%	[12, 16]
	u_{19}	Thickness of the armour bedding	mm	1.5	[1.425, 1.575]	± 5%	[12, 16]
	u_{20}	Thickness of the armour	mm	6	[5.7, 6.3]	± 5%	[12, 16]
	u_{21}	Thickness of the outer serving	mm	4.5	[4.275, 4.725]	± 5%	[12, 16]
	u_{22}	Earth resistivity (sand with seawater)	Ωm	–	[0, 500]	–	[17]
	u_{35}	Fault location along the transmission line	km	–	[0, 54]	–	–

togram of Fig. 4) is due only to u_{22}, u_{35}, and u_{13}. While the randomness of the fault location (u_{35}) obviously greatly affects the distance protection performance ($T_{u_{35}} = 0.483$), its overall importance is, interestingly, smaller than the ρ of the submarine cable ρ_{SM} (u_{22}), which is the most influential input parameter ($T_{u_{22}} = 0.529$). In particular, the uncertainty of ρ_{SM} contributes, alone, to around 38% of the variability of the fault location error ($S_{u_{22}} = 0.379$). The tolerance of the submarine cable conductor radius (u_{13}) has an impact of less than 10%. Also, around 15% of the variability of the fault location error is due to the interaction among ρ_{SM} and the fault location ($S_{u_{22},u_{35}} = 0.152$). Remarkably, the state-of-the-art one-at-a-time SA conducted in [5], [11], and [12] would fail in capturing such non-negligible interactive effect.

Since reducing the variability of the most important parameters would lead to the biggest enhancement in the IED performance, the attained results provide TSOs with directions about which factors deserve special attention in order to reduce the overall IFL algorithm error. If, on the one hand, the randomness of the fault location is "uncontrollable", on the other hand the tolerance of the conductor radius and the uncertainty of ρ can be somehow "controlled". In particular, since ρ_{SM} ranks first in terms of importance, it can be derived that the properties of the medium surrounding the submarine cable are worth better characterization, e.g., via direct measurement. As accurately estimating/measuring the soil characteristics might be complex (especially in the case of the submarine cable sections), an alternative action would be indirectly identifying the "optimal" value of ρ, i.e., by measuring the actual line impedance with field short-circuit tests [9] or retrieving it from fault records after known events [7].

Moreover, the routine adoption of a single value for ρ (e.g., 100 Ωm [5]) might easily undermine the IED performance in the case it is not representative of the physical properties of the surrounding medium. This is proven by comparing the three histograms of Fig. 5, where: (a) the magenta histogram is the distribution of ϵ with $\rho_{SM} \in [0, 500]$ Ωm; (b) the green histogram is the distribution of ϵ after conducting a further MCS with ρ_{SM} fixed at the "optimal" value (260 Ωm), i.e., the value of ρ_{SM} that leads to the smallest fault location error ϵ; (c) the blue histogram is the distribution of ϵ after conducting a further MCS with ρ_{SM} fixed at 100 Ωm, i.e., the "default" value of ρ_{SM} commonly adopted for the whole transmission line [5]. When $\rho_{SM} \in [0, 500]$ Ωm, the maximum error is around −2 km. If $\rho_{SM} = 260$ Ωm, the IFL algorithm performs way better, with a maximum error of around −500 m. However, if $\rho_{SM} = 100$ Ωm, the IFL algorithm performance is worse than not only when $\rho_{SM} = 260$ Ωm (green histogram), but also when ρ_{SM} is left free to vary (magenta histogram). This underscores that improperly fixing an important input parameter (e.g., here, setting ρ_{SM} at a value that does not accurately reflect the properties of the surrounding medium) might degrade the IFL algorithm accuracy even more than when the same input parameter is considered uncertain.

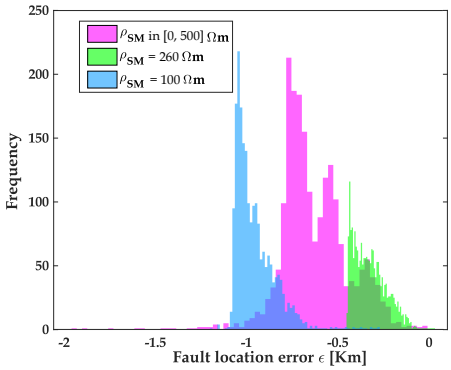

Figure 5: Performance of the IFL algorithm with the cable modelling approach 2, where $\rho_{SM} \in [0, 500]$ Ωm (magenta), $\rho_{SM} = 260$ Ωm (green), and $\rho_{SM} = 100$ Ωm (cyan).

Table 2 shows that the total effect SIs of all the other 32 parameters are null: these, although uncertain, do not affect the distance protection performance. Hence, these parameters would need no refinement or corrective action, and could be fixed at any value within their variation range (e.g., at their nominal ones) with no impact on the IFL algorithm accuracy, so to reduce the total number of parameters under study.

Table 2: VBSA for approach 2 with variable fault location.

Input Name	First-order SI	Total effect SI
u_{22}	0.379 ± 0.030	0.529 ± 0.031
u_{35}	0.333 ± 0.029	0.483 ± 0.031
u_{13}	0.073 ± 0.017	0.089 ± 0.017
$\mathbf{u} \setminus \{u_{13}, u_{22}, u_{35}\}$	0.000 ± 0.000	0.000 ± 0.000

8 Conclusions

This paper conducts SA to thoroughly investigate which are the most important parameters affecting the performance of the distance protection in a submarine transmission system. Among all the investigated parameters (i.e., the geometry and the cross-section of the cables, the properties of the surrounding medium, and the cable model), the earth resistivity ρ of the submarine cable section turns to be the most influential one. This leads to recommend that ρ is worth better characterization (e.g., via direct or indirect measurement) to enhance the performance of distance protection algorithms. In fact, computing the line impedance (in particular, the zero sequence component) with a more accurate value of ρ would allow calculating more accurate IED settings, hence ultimately leading to the highest increase in the IED performance accuracy.

Also, the choice of using default values for ρ (e.g., 100 Ωm as per common practice) should be carefully considered: the value of ρ specifically used might, in fact, degrade the distance protection performance if it does not trustworthily represent the realistic conditions of the surrounding medium.

Furthermore, the cable model of the available EMT software tools used to compute the reference sequence impedances of the line can represent, already on its own, a non-negligible source of error for distance protection algorithms, if it does not properly reflect the real characteristics of the cable system.

9 Acknowledgments

This work was supported by the Interoperability Network for the Energy Transition (IntNET), which is a project funded by the European Union's Horizon Europe Research and Innovation Program (Grant 101070086).

References

[1] Ardelean, M. and Minnebo, P., *HVDC Submarine Power Cables in the World*. Luxembourg: Publications Office of the European Union, 2015.

[2] Jensen, C., Faria da Silva, F., Bak, C. L., et al., "Switching studies for the Horns Rev 2 wind farm main cable," in *Proc. Int. Conf. Power Systems Transients, IPST 2011*, Delft University Press, June 2011.

[3] Wang, W., Yan, X.. Li, S., et al., "Failure of submarine cables used in high-voltage power transmission: Characteristics, mechanisms, key issues and prospects," *IET Generation, Transmission & Distribution*, vol. 15, no. 9, pp. 1387–1402, 2021.

[4] Bawart, M., Marzinotto, M. and Mazzanti, G, "A deeper insight into fault location on long submarine power cables," *Elektrotechnik und Informationstechnik*, vol. 131, pp. 355–360, 2014.

[5] Das, S., Santoso, S., Gaikwad, A., et al., "Impedance-based fault location in transmission networks: theory and application," *IEEE Access*, vol. 2, pp. 537–557, 2014.

[6] Ziegler, G., *Numerical Distance Protection: Principles and Applications*. Wiley, 2008.

[7] Amberg, A., Rangel, A. and Smelich, G., "Validating transmission line impedances using known event data," in *2012 65th Annual Conference for Protective Relay Engineers*, pp. 269–280, 2012.

[8] Gustavsen, B., Martinez, J.A. and Durbak, D., "Parameter determination for modeling system transients-Part II: Insulated cables," *IEEE Transactions on Power Delivery*, vol. 20, no. 3, pp. 2045–2050, 2005.

[9] Sellwood, V., Klapper, U., Kruger, M., et al., "A new technique for setting distance protection and fault location by measurement of transmission line system impedance characteristics," in *8th IEE Int. Conf. AC and DC Power Transmission*, pp. 197–199, 2006.

[10] Ginocchi, M., Ponci, F. and Monti, A., "Sensitivity Analysis and Power Systems: Can We Bridge the Gap? A Review and a Guide to Getting Started," *Energies*, vol. 14, no. 24, 2021.

[11] Tsimtsios, A. M. and Nikolaidis, V. C., "Setting zero-sequence compensation factor in distance relays protecting distribution systems," *IEEE Trans. Power Deliv.*, vol. 33, no. 3, pp. 1236–1246, 2018.

[12] Johannesson, N. and Norrga, S., "Sensitivity of Cable Model Parameters for Traveling Wave Differential Protections in MTDC Systems," *IEEE Trans. Power Deliv.*, vol. 35, no. 5, pp. 2212–2221, 2020.

[13] Ginocchi, M., Penthong, T., Ponci, F., et al., "Statistical design of experiments for power system protection testing: A case study for distance relay performance testing," *IEEE Access*, vol. 12, pp. 27052–27072, 2024.

[14] Das, S., Ananthan, S. N. and Santoso, S., "Estimating zero-sequence line impedance and fault resistance using relay data," *IEEE Trans. Smart Grid*, vol. 10, no. 2, pp. 1637–1645, 2019.

[15] Nexans Norway AS, *Technical Description of 115 kV XLPE Land Cable - single core*, 2009.

[16] Nexans Norway AS, *Technical Description of 115 kV XLPE Submarine Cable - three core*, 2009.

[17] Pandey, L. M. S., Shukla, S. K. and Habibi, D., "Electrical resistivity of sandy soil," *Géotechnique Letters*, vol. 5, no. 3, pp. 178–185, 2015.

[18] Shao Q., Younes A., Fahs M. et al., "Bayesian sparse polynomial chaos expansion for global sensitivity analysis," *Comput. Methods Appl. Mech. Eng.*, vol. 318, pp. 474–496, 2017.